Probes of heterogeneity in rotational dynamics: Application to supercooled liquid CS_2

Joohyun Kim, Wu-Xiong Li,* and T. Keyes
Department of Chemistry, Boston University, Boston, Massachusetts 02215
(Received 9 July 2002; published 27 February 2003)

The distribution of individual molecular contributions to the second-rank rotational correlation function is introduced and used to construct probes of heterogeneity in rotational dynamics. The ideas are tested in a molecular dynamics simulation of supercooled liquid CS_2. Both the quantity of heterogeneity and its lifetime or exchange time τ_{ex} increase as the temperature is lowered through the supercooled state, and increase strongly as the mode-coupling temperature T_c is approached. Crossover from Arrhenius to super-Arrhenius behavior of the rotational relaxation times τ_1 and τ_2 is observed, direct evidence of fragility in CS_2. The T dependence of τ_{ex} is stronger than that of the rotational times, and it may approach them from below at T_c, although the simulation is then very difficult. A detailed characterization of other aspects of the dynamical crossover is obtained, and the general implications of rotational heterogeneity for supercooled dynamics are discussed.

DOI: 10.1103/PhysRevE.67.021506 PACS number(s): 64.70.Pf, 64.60.Ht, 61.20.Lc, 61.43.Fs

I. INTRODUCTION

Recently developed experimental techniques allow an observation of appropriately selected sub ensembles or even individual molecules in liquids [1–4]. They indicate that supercooled liquids are dynamically heterogeneous, with distinct regions of fast and slow relaxation which persist for a characteristic lifetime or exchange (in the sense that heterogeneity relaxes by exchange of properties among neighbor regions) time τ_{ex} [1,2]. Molecular dynamics (MD) simulation studies have helped to reveal the underlying microscopic details [5–12]. However, in spite of the promise of the MD method, a very large gap still exists between the time scale accessible to computation and that probed by experiments; simulation of deeply supercooled liquid states remains an outstanding challenge [13]. Also, while the experiments mainly measure rotational dynamics, the simulations have focused on the translational heterogeneity observable in simple atomic systems such as the binary Lennard-Jones mixture. Only a small number of studies on molecular reorientation in supercooled liquids are found in the literature [14,15]. The goal of this paper is to connect more closely with experiments by simulating rotational dynamics in the highly polarizable molecular system CS_2, while evaluating and analyzing some new probes of heterogeneity.

Generally, heterogeneity found in the supercooled state represents a deviation from the homogeneous dynamics occurring in normal liquids. In contrast to the conventional view where all molecules behave the same, each molecule is assigned a distinct relaxation time. Experimentally, it has been reported that molecules only several nanometers apart can differ by orders of magnitude in relaxation time, even though no clear structural difference can be identified [1]. Well-defined average times for the whole system can still be calculated, but they become less useful with increasing heterogeneity, and it is essential to find ways to probe individual molecules. Moreover, heterogeneous dynamics is not static. After some interval, ''relaxation of the relaxation,'' possibly due to an exchange mechanism, changes the molecular properties [16,17]. Thus, the dynamical slowing down in supercooled liquids is inextricably tied up with heterogeneity.

The most fundamentally interesting aspect of heterogeneity is its possible control of other dynamical processes. For example, it has been argued that the breakdown of the Stokes-Einstein law, stretched exponential behavior of time correlation functions, and the change from Arrhenius to super (stronger than)-Arrhenius T dependence of relaxation times in fragile liquids are all caused by heterogeneity [1,2,18–20]. Nevertheless, many details are not well understood. What causes heterogeneous dynamics? How is it connected to other phenomena and characteristic temperatures of the deeply supercooled state and the glass? Do translational and rotational dynamics provide the same information about heterogeneity? May it be related to features of the potential energy surface, or *landscape* [21]?

In the following, we introduce a scheme for the characterization of dynamic rotational heterogeneity via the distribution of individual molecular contributions to the anisotropic polarizability correlation function. In Sec. II we define new quantities which clearly highlight rotational heterogeneity. Section III describes the details of the simulation. In Sec. IV, T-dependent rotational relaxation of $\rho = 1.46$ g/cm^3 isochoric CS_2 is investigated, and the new indicators of heterogeneity are evaluated, tested, and discussed. Our conclusions, and a summary of the significant temperatures for the dynamical crossover in this system, are presented in Sec. V.

II. CHARACTERIZATION OF DYNAMIC HETEROGENEITY IN ROTATIONAL DYNAMICS

Time-dependent properties of liquids are most commonly calculated as correlation functions incorporating an average over all the molecules. The simplest correlations involve two variables and, due to time-translation invariance, a single time argument. Such functions cannot distinguish between

*Current address: Applied Biosystems Inc., 850 Lincoln Center Drive, Foster City, CA 94040.

homogeneous and heterogeneous systems. For example, as has been much discussed, with a rotational correlation function alone there is no way to differentiate between homogeneous and heterogeneous molecular mechanisms for stretched exponential t dependence [17]. More complicated multipoint, multitime correlations have been proposed as indicators of translational heterogeneity [22,23]. Averaging a product of two variables discards much molecular informations. On the other hand, distributions are averages which incorporate all product averages as moments. In the following we demonstrate that the rotational heterogeneity is revealed by the distribution of the individual molecular contribution to the correlation function.

Rotational motion is often observed via the coupling of the molecular polarizability to an external field [24]. For rigid molecules and ignoring dipole-induced dipole effects, rotational dynamics and polarizability dynamics are equivalent, and we will discuss them interchangeably in the following. Even so cross correlations (pair contributions) enter the polarizability correlation, but only complicate an attempt to study heterogeneity. Thus we begin with the single-particle anisotropic polarizability correlation function $C_\phi(t)$ and its i'th molecular contribution $\phi_i(t)$,

$$C_\phi(t)=\left\langle \frac{1}{N}\sum_{i=1}^{N}\phi_i(t)\right\rangle \Big/ \left\langle \frac{1}{N}\sum_{i=1}^{N}\phi_i(0)\right\rangle, \tag{1}$$

$$\phi_i(t)=\mathrm{Tr}\{\boldsymbol{\alpha}_i^{(2)}(t)\cdot\boldsymbol{\alpha}_i^{(2)}(0)\}, \tag{2}$$

where the anisotropic molecular polarizability is defined as $\boldsymbol{\alpha}_i^{(2)}=\boldsymbol{\alpha}_i-\frac{1}{3}(\mathrm{Tr}\boldsymbol{\alpha}_i)\mathbf{1}$, $\boldsymbol{\alpha}_i$ is the polarizability of the i'th molecule, $\mathbf{1}$ is the unit 3×3 matrix and N is the number of molecules. All the molecules make identical contributions to each of the two sums in Eq (1) (for a pure liquid), and that is why heterogeneity cannot be studied with C_ϕ.

In the case of rigid linear molecules $C_\phi(t)=(\Delta\alpha)^2C_2(t)$, where $C_2(t)$ is the second-rank rotational correlation function and $\Delta\alpha$ is the polarizability anisotropy. Our system, CS_2, can be modeled as a rigid linear molecule. Thus in the following we set $\Delta\alpha$ equal to unity. In general $C_l(t)=1/N\Sigma_{i=1}^{N}\langle P_l(\vec{u_i}(t)\cdot\vec{u_i}(0))\rangle$, where $P_l(x)$ is the Legendre polynomial of order l, and $\vec{u_i}$ is the molecular axis vector.

The central quantity presented in this paper is the distribution of molecular contributions to the rotational or polarizability correlation,

$$P(\phi,t)=\left\langle \sum_{i=1}^{N}\delta(\phi-\phi_i(t))\right\rangle. \tag{3}$$

The first moment is, except for a normalization factor, $C_\phi(t)$, but $P(\phi,t)$ contains far more information. In fact, a very useful way to study the T dependence of heterogeneity is to maintain a *constant* C_ϕ, that is, at each temperature, $P(\phi,t)$ is evaluated at the time $t(C,T)$ which yields a chosen value of C_ϕ. Furthermore, fortuitously, $P(\phi,t)$ is a delta function for molecules which have not relaxed at all and also shows a distinct, well-separated peak for molecules with complete reorientational randomization. Thus, as will be seen next, $P(\phi,t)$ is well suited for distinguishing ''fast'' and ''slow'' molecules.

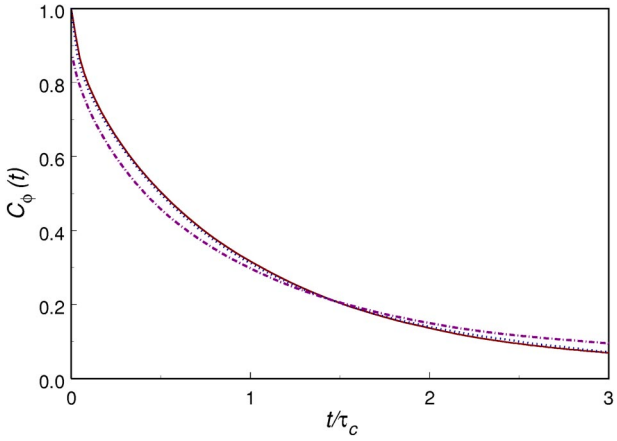

FIG. 1. Normalized single-particle anisotropic polarizability correlation function $C_\phi(t)$ vs t/τ_c at $T=180$ K (solid), $T=165$ K (dotted), and $T=120$ K (dot dashed) for $P=1$ atm.

We now illustrate the method. Three temperatures at $P=1$ atm studied in previous work are chosen [25]. Higher temperatures 180 K and 165 K are representative of homogeneous behavior, and heterogeneity is clearly visible at 120 K. Figure 1 shows the polarizability correlation $C_\phi(t)$ for the three T. To best compare the data at different T, the time axis is scaled with the rotational correlation time τ_c, defined as follows: The rotational correlation function has (Fig. 1) an initial fast decay that is not relevant to the slow relaxation of interest here, so it is discarded. Then, $C_\phi(t)$ in the range of $0.8\geqslant C_\phi(t)\geqslant0.1$ is redefined as $C_\phi(t)/0.8$ and fitted to a stretched exponential, and

$$\tau_c=\int_0^\infty dtC_\phi(t); \tag{4}$$

τ_l is obtained similarly ($\tau_c\equiv\tau_2$).

By comparing distributions at different T and constant C_ϕ we observe dynamical changes under conditions where, by definition, the correlation function shows none. In Fig. 2, $P(\phi,t)$ is plotted at the three temperatures for times such that $C_\phi(t)$ is 0.8, 0.6, 0.3, and 0.2. The range ϕ is $2/3\geqslant\phi\geqslant-1/3$. For rigid molecules $P(\phi,t=0)=\delta(\phi-2/3)$, but in our model of flexible CS_2 it has a finite width. We calculate the polarizability with the ''point atomic polarizability approximation'' and the anisotropy changes with the internal coordinates [26]. Here, for simplicity, we treat the molecules as having the equilibrium geometry and an orientation along the vector between the two S atoms, restoring the delta function. In this fashion we might miss some short time dynamics, but nothing on the time scale of interest.

A molecule that experiences small angular displacement from its initial orientation will have $\phi\sim2/3$. Thus for $t\geqslant\tau_c$, when a substantial fraction of molecules have been randomized, $\boldsymbol{\phi\sim2/3}$ **indicates a slow molecule**. Of course even with complete relaxation a molecule may revisit its original orientation, but given a significant population of

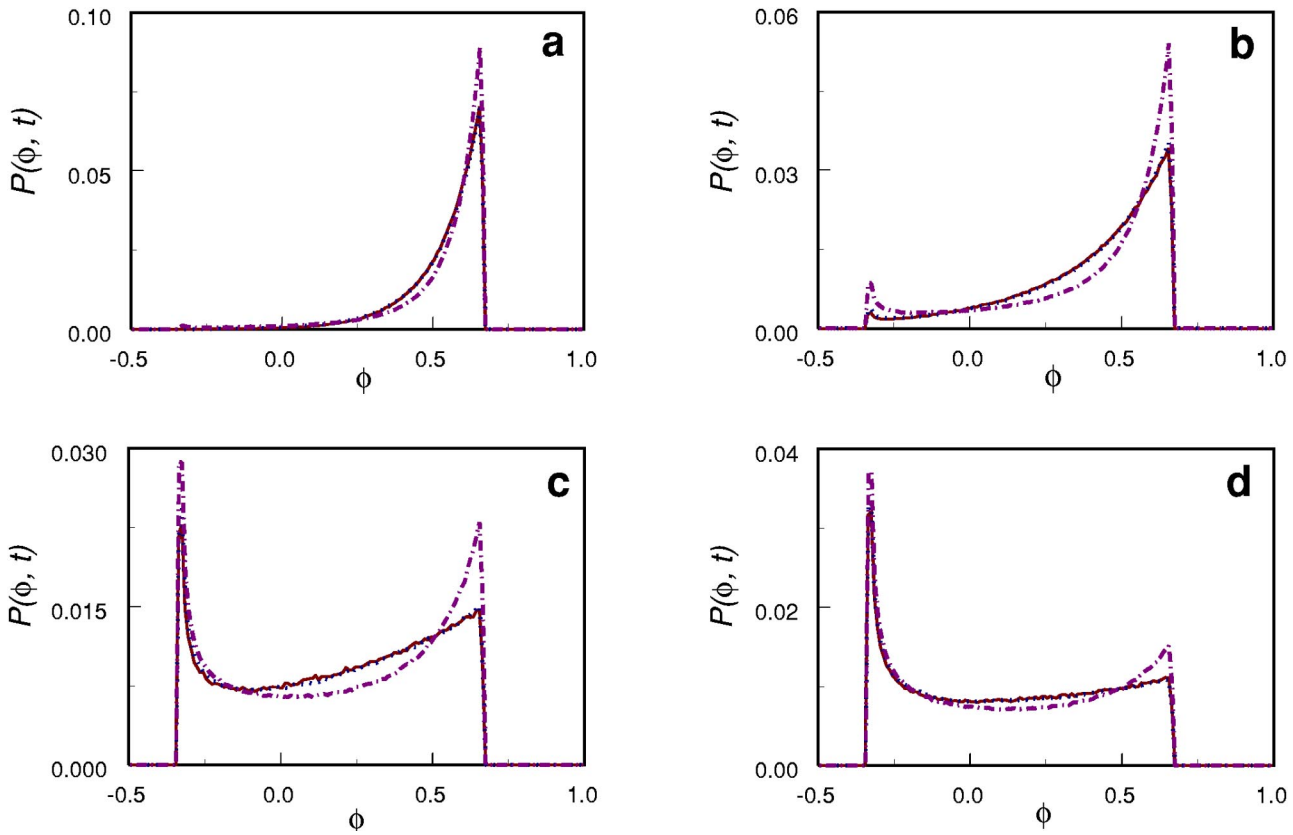

FIG. 2. Distributions $P(\phi,t)$ at $T=180$ K (solid), $T=165$ K (dotted), and $T=120$ K (dot dashed) for $P=1$ atm. From (a)–(d), $C_\phi(t)=0.8$, 0.6, 0.3, and 0.2, respectively.

slow molecules they will predominate at $\phi\sim 2/3$. For $t\ll\tau_c$ all molecules have $\phi\sim 2/3$ and it is not significant. At very long times, measurement becomes difficult and both slow and fast molecules become relaxed, so $P(\phi,t)$ is most informative at $t\approx\tau_c(T)$.

The 120 K distributions are clearly different from the two indistinguishable curves at 165 K and 180 K. All $P(\phi,t(C,T))$, for fixed C, collapse onto a single master curve at high T. Observation of $C_\phi(t,T)$ (Fig. 1) might provide indirect evidence of heterogeneity at low temperature through the more fully developed stretched exponential pattern at 120 K. On the other hand, the distribution of the molecular contributions at 120 K plainly shows the existence of a larger proportion of slow molecules with $\phi\sim 2/3$ and fast molecules with $\phi\sim -1/3$, confirming the rotational heterogeneity without ambiguity. Quantitative measures of heterogeneity can be constructed in terms of deviations of $P(\phi,t(C,T))$ from the high-T master curve, which defines homogeneous dynamics. Here we propose a simple indicator of the root-mean-square *amplitude* of heterogeneity,

$$\Delta_{het}(T)=\left\{\int_{-1/3}^{2/3} d\phi\,(P(\phi,\tau_c,T)-P(\phi,\tau_c,T_{hi}))^2\right\}^{1/2}, \tag{5}$$

where T_{hi} is the reference high temperature and $P(\phi,\tau_c,T)$ represents $P(\phi,\tau_c)$ obtained at T.

Since the heterogeneity revealed in recent experiments is not static—slow molecules do not remain slow forever—we also seek information about the lifetime. Following ideas from multidimensional NMR [3], we perform a ''measurement'' of $P(\phi,t)$, let the system evolve for waiting time t_w, and calculate $P(\phi,t)$ again to determine if slow molecules are still slow, or have been thermalized. The relevant conditional probability density is denoted as $P_c(\phi_1,\phi_2,t,t_w)$ and is defined as follows: given a molecule with $\phi=\phi_1$ in a measurement over the time interval $(0,t)$, $P_c\,d\phi_2$ is equal to the probability that ϕ of the molecule falls in the range $(\phi_2,\phi_2+d\phi_2)$ measured over a second time interval (t_w,t_w+t), following the relaxation of the system for time t_w. Note that the waiting interval begins at zero, not t.

With the quantity P_c, dynamic heterogeneity can be differentiated from static heterogeneity. Consider first the two limiting cases. In the static limit of infinitely long-lived heterogeneity there is no waiting time dependence and slow molecules are always slow, so

$$P_c(\phi_1,\phi_2,t,t_w)\approx\delta(\phi_2-\phi_1),\phi_1,\phi_2\to 2/3,t\geqslant\tau_c. \tag{6}$$

The delta correlation does not hold when substantial relaxation has occurred because of the stochastic nature of the dynamics. At the other extreme, in the homogeneous limit P_c has neither t_w dependence nor, since all molecules are equivalent, ϕ_1 dependence,

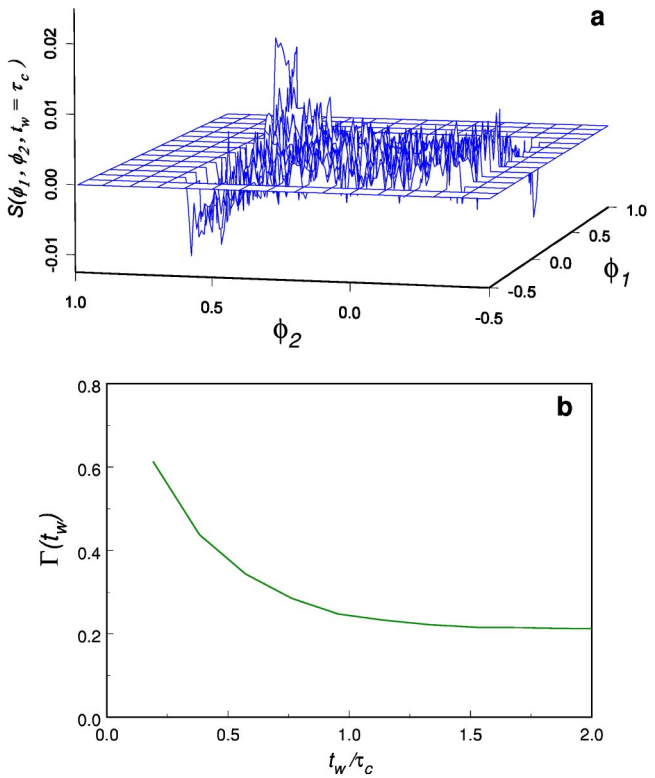

FIG. 3. (a) Two-dimensional plot of $S(\phi_1,\phi_2,t_w)$ for $T=120$ K, $P=1$ atm, $t_w=524$ ps$=\tau_c$, (b) time profile of $\Gamma_{het}(t_w)$ vs t_w/τ_c.

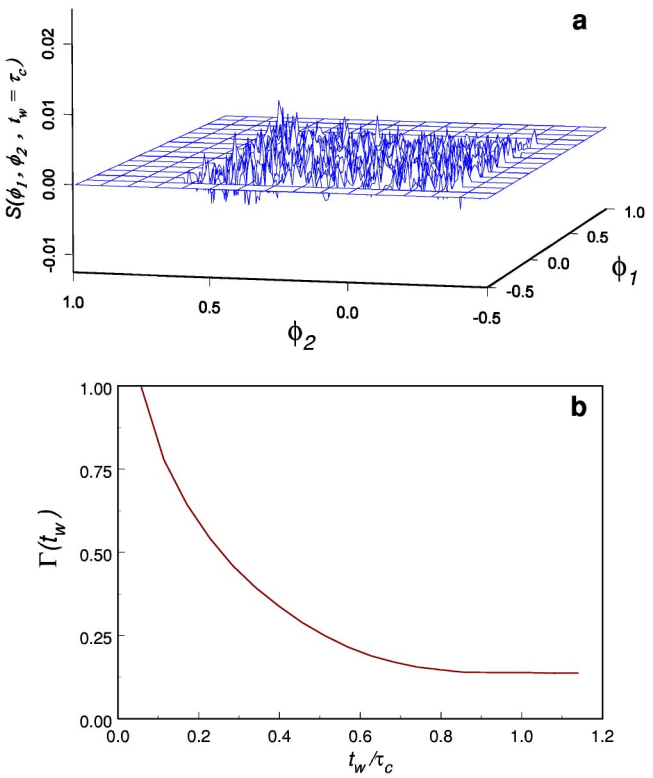

FIG. 4. As in Fig. 3 for $T=180$ K, $P=1$ atm.

$$P_c(\phi_1,\phi_2,t,t_w)=P(\phi_2,t). \tag{7}$$

As with deviations of P from its high-T limit, deviations of P_c from Eq (7) indicate the presence of heterogeneity, and the t_w dependence will yield its lifetime, τ_{ex}. Thus we define the difference

$$S(\phi_1,\phi_2,t_w)=P_c(\phi_1,\phi_2,\tau_c,t_w)-P(\phi_2,\tau_c) \tag{8}$$

as a quantity which vanishes in the absence of heterogeneity, and we define a lifetime indicator $\Gamma_{het}(t_w)$,

$$\Gamma_{het}(t_w,T)=\left\{\int_{-1/3}^{2/3}d\phi_1\int_{-1/3}^{2/3}d\phi_2 S^2(\phi_1,\phi_2,t_w,T)\right\}^{1/2}, \tag{9}$$

which will vanish for $t_w \gg \tau_{ex}$. Here we again choose $t=\tau_c$ for maximum visibility of the heterogeneity.

Figures 3(a) and 4(a) are two-dimensional plots of $S(\phi_1,\phi_2,t_w=\tau_c)$ for 120 K and 180 K, respectively; τ_c is also a natural choice of t_w. Any nonzero feature, a peak or a negative "well," indicates that molecules remember their rotational relaxation time on the time scale of τ_c; because of long-lived heterogeneity some part of the distribution does not reach its asymptotic value. Clearly, since no distinct peaks are visible in Fig. 4(a), the 180 K system is homogeneous in the time scale of τ_c. Data at 165 K that are not shown here exhibit the same behavior. On the other hand, at 120 K we find a strong peak in the region of the slow molecules; *slow molecules remain slow even after waiting for a time* τ_c. Thus, high temperatures are revealed as homogenous cases and the low temperature, 120 K, appears with dynamic heterogeneity in the rotational dynamics.

TABLE I. Low-temperature MD runs; the only three trajectories reaching over 100 ns before crystallization at 80 K and 75 K. t_{traj} is the interval for data analysis, t_{eq} is the equilibration time before data analysis, and Δt is the size of "intermolecular" time step. τ_l^β and β_l are parameters for fit of C_l to stretched exponential $\exp[-(t/\tau_l^\beta)^{\beta_l}]$. τ_l is a corresponding correlation time obtained by integration as explained in Sec. II.

Temp.(K)	t_{traj} (ns)	t_{eq} (ns)	Δt (fs)	τ_2^β (ps)	β_2	τ_2 (ps)	τ_1^β (ps)	β_1	τ_1 (ps)
80[a]	240	40	10	4172	0.48	9035	6699	0.64	9313
80[b]	80	20	10	1994	0.78	2301	3461	0.92	3599
75	180	20	10	5243	0.82	5840	8307	0.92	8546

[a]Run I.
[b]Run II.

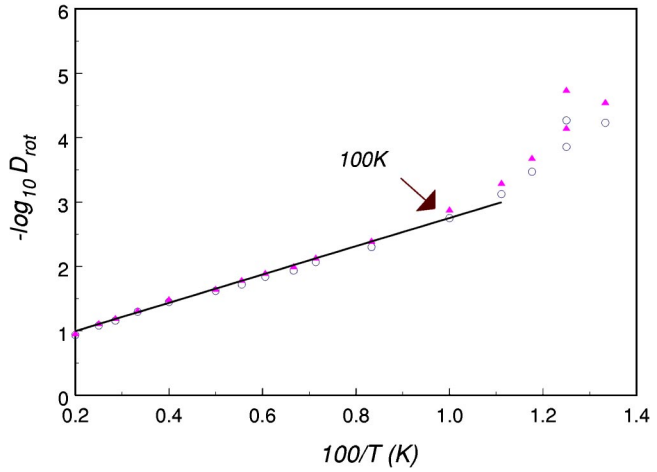

FIG. 5. Arrhenius plots of D_{rot}, obtained from $C_2(t)$ (triangles) and $C_1(t)$(circles) with Debye formula, $D_{rot}=[l(l+1)\tau_l]^{-1}$, for $\rho=1.46$ g/cm^3 and 500 K$\geqslant T\geqslant$75 K. Time unit for τ_1 and τ_2 is in picosecond. Data from run I and run II, 80 K, are shown together. The arrow at 100 K indicates a possible crossover to super-Arrhenius behavior.

The decay of the heterogeneity, normalized to unity at an arbitrary short time after the initial fast drop, is shown in Figs. 3(b) and 4(b). We identify the correlation time of $\Gamma_{het}(t_w)$ with τ_{ex}. After discarding the initial decay, τ_{ex} is calculated with

$$\Gamma_{het}(t_w)=A+B\exp(-t_w/\tau_{ex}). \tag{10}$$

Generally, if the trajectory is sufficiently long to give a well averaged $C_\phi(t)$, Eq (10) is well obeyed. In fact, τ_{ex} is not strictly the lifetime of the local environment. Since rotational relaxation is not coherent motion, in general $\phi_2\neq\phi_1$ even with static heterogeneity. However, as long as we focus on the time scale of τ_c, τ_{ex} is a good representation for the lifetime and the exchange time.

In sum, our new probes of heterogeneity are $P(\phi,t)$ and $S(\phi_1,\phi_2,t_w)$ and the corresponding integrated quantitative measures Δ_{het} and $\Gamma_{het}(t_w)$. They will be evaluated for supercooled CS_2 in Sec IV.

III. COMPUTATIONAL DETAILS

The system we investigate is 1.46 g/cm^3 isochoric CS_2, $N=108$, from the normal liquid state down to 75 K. At $P=1$ atm, 1.46 g/cm^3 is the density at the melting temperature of 165 K, so $T<165$ K is supercooled. The potential is Tildesley-Madden [27] model "*C*" of atom-atom intermolecular Lennard-Jones interactions, plus harmonic bends and stretches including a coupling of the two C-S stretches.

Trajectories are obtained using both *NVT* and *NVE* ensembles. For *NVT* we use our previous implementation, Hoover-Evans constraint dynamics on the center of mass kinetic energy [28,25]. For the lowest temperatures, 80 K and 75 K, the faster *N-V-E* method with velocity scaling every 1000 time steps is applied. Down to 85 K, it was verified that *NVE* and *NVT* give essentially equivalent results. The internal degrees of freedom are handled with the multiple time step algorithm, where the time step for the fast intramolecular degrees of freedom is 10 times smaller than that for the intermolecular interactions. The intermolecular time step is 1 fs for $T>120$ K, 5 fs for 120 K$\geqslant T\geqslant$85 K, and 10 fs for 80 K and 75 K. At 90 K, we confirmed that 10 fs and 5 fs give the same results. Other details can be found in previous work [25].

For $T\geqslant$85 K well averaged results for all the quantities of interest are easily obtained with no special procedures. However, at 80 K and 75 K simulation becomes problematic due to the abrupt increase in relaxation time and consequent difficulty in averaging, the possibility of crystallization, and nonergodicity. The computational requirements are then more rigorous, specifically, long trajectories for good averaging over the configurations available to a single MD run, long equilibration periods to compensate for slow "aging," and many runs with uncorrelated initial configurations for ergodicity. Here, we use two long runs at 80 K, denoted I and

TABLE II. Stretched exponential parameters, the ratio τ_1/τ_2, and the exchange time τ_{ex}. τ_l^β and β_l ($l=1$ or 2) are parameters for the stretched exponential $\exp[-(t/\tau_l^\beta)^{\beta_l}]$. τ_1, τ_2, and τ_{ex} are obtained as explained in Sec. II.

Temp.(K)	τ_2^β (ps)	β_2	τ_1^β (ps)	β_1	τ_1/τ_2	τ_{ex}
300	3.17	0.88	9.69	0.96	2.92	
250	4.64	0.86	13.87	0.97	2.80	
200	6.90	0.89	20.45	0.96	2.85	
180	9.49	0.89	26.2	1.0	2.61	
165	12.1	0.88	34.2	0.98	2.67	3.03
150	16.5	0.89	45.0	0.99	2.63	4.21
140	20.5	0.89	55.2	0.98	2.61	5.47
120	38	0.88	99	0.97	2.46	11.73
100	114	0.85	277	0.96	2.27	42.61
90	296	0.84	651	0.94	2.07	117.30
85	693	0.79	1406	0.90	1.87	

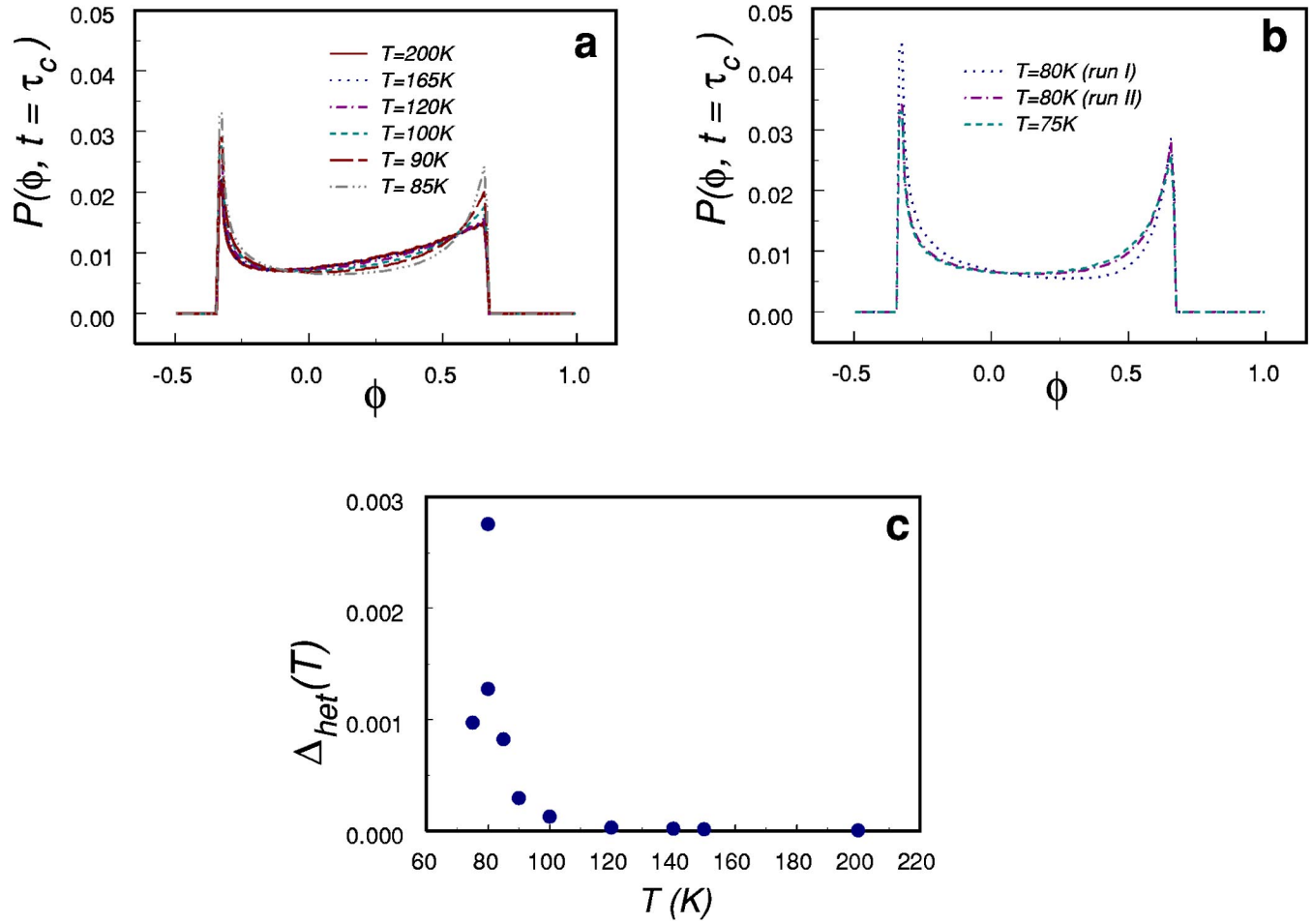

FIG. 6. T-dependent rotational heterogeneity, $\rho=1.46$ g/cm^3. Distributions $P(\phi,t=\tau_c)$ are shown in (a) (200 K$-$85 K) and (b) (the low temperatures 80 K and 75 K); (c) is root-mean-square heterogeneity Δ_{het} with reference temperature 165 K.

II, and one at 75 K, summarized in Table I. The runs at 80 K and 75 K can be regarded as segments of the ideal long trajectory. We believe that the two runs at 80 K reveal two distinct types of dynamical behavior characteristic of deeply supercooled states.

Preparation of the initial configuration has been explained elsewhere [25]. The simulation begins at 1000 K and then the temperature is dropped to 500 K for more equilibration. Finally at the temperature of interest the system is equilibrated for approximately $10\tau_c$ before data gathering. At lower temperatures, equilibration is hard to achieve because of aging, and a quantitative criterion for a safe starting point for data gathering should be employed based upon, e.g., nonequilibrium artifacts in pressure, potential energy, or wave vector dependent structural quantities. However, for this work, simply monitoring the potential energy and visualizing the configuration with a graphic viewer (VMD) should be sufficient [29]. Above 85 K there is no difficulty.

For good averaging the trajectory length is chosen to be about 100 τ_c. At least two trajectories with the same length are used to check for confidence of the run length for $T\geqslant 85$ K. Again, for 80 K and 75 K, this is not possible because of crystallization. The runs used at these temperatures (Table I) are simply the longest ones we could obtain.

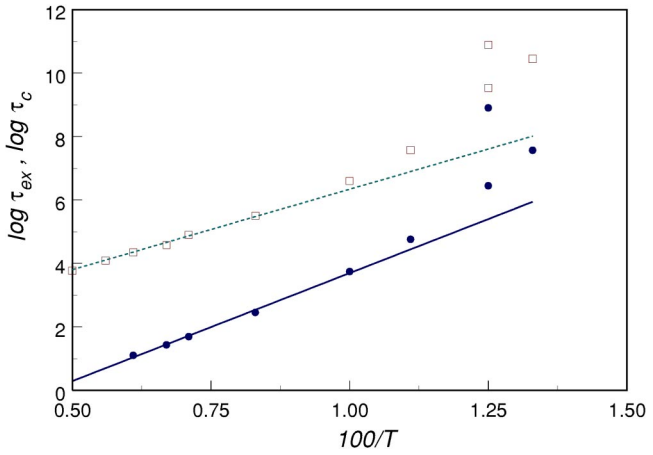

FIG. 7. T-dependence of the exchange time τ_{ex} (circles) and τ_c (open squares). Time unit is picosecond, $\rho=1.46$ g/cm^3. Lines are least square fits to the linear Arrhenius regime. Activation energy E_A for τ_{ex} over 165 K$\geqslant T\geqslant$120 K is 680 K, and E_A for τ_2 over 500 K$\geqslant T\geqslant$120 K is 506 K.

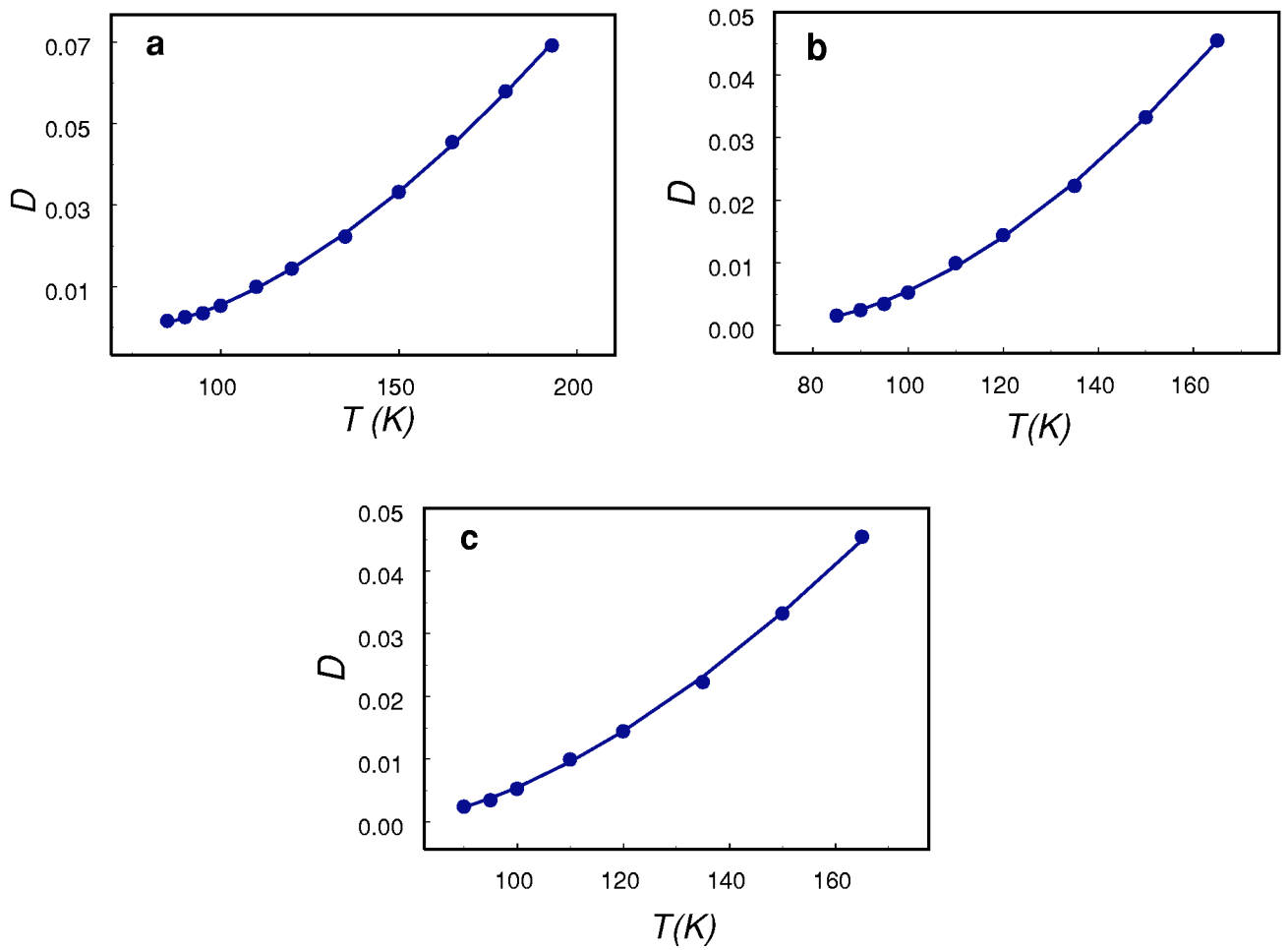

FIG. 8. Estimation of T_c with the power-law mode coupling formula for D (Å^2/ps) using three different temperature ranges, $\rho = 1.46$ g/cm^3; for (a)–(c), 193 K$\geqslant T \geqslant$85 K, 165 K$\geqslant T \geqslant$85 K, and 165 K$\geqslant T \geqslant$90 K, respectively. Points are MD results, lines are fits.

IV. DYNAMICAL SLOWING DOWN AND TEMPERATURE DEPENDENT ROTATIONAL HETEROGENEITY

Angell has argued that CS_2 is very fragile and has estimated a glass transition temperature $T_g = 92$ K, $P = 1$ atm [21]. Although we are considering a constant density, our 165 K system has $P = 1$ atm and relaxation times have increased by perhaps three decades from room temperature. Only pronounced super-Arrhenius T dependence can yield $T_g = 92$ K. Figure 5 displays Arrhenius plots of $l(l+1)\tau_l$ for $l = 1,2$, with τ_l determined from $C_2 = C_\phi$ and C_1 as indicated. In the Debye limit of small step rotational diffusion the quantity plotted equals the inverse of the rotational diffusion coefficient $1/D_{rot}$. Such plots provide the conventional characterization of T-dependent rotational relaxation. Stretched exponential parameters for the time correlation functions at each temperature, used in the calculation of τ_1 and τ_2, are shown in Tables I and II. Super-Arrhenius behavior is evident below 90 K. If this pattern persists to T_g, and if the rotational times remain connected to the viscosity as indicated by experiment in other systems, we can confirm, by simulation, that CS_2 is a fragile liquid.

The super-Arrhenius character of τ_2 is somewhat stronger than that of τ_1, even though they are governed by the same reorientational process. The reason is that C_2 is more easily relaxed by small angular steps than is C_1. With decreasing T the dynamics changes (*vide infra*) towards larger steps, providing an additional (relative to τ_1) slowing down for τ_2. Such a small effect would be negligible with many decades of relaxation, but cannot be ignored within the limited dynamic range of a simulation. Activation energies from the linear part of Fig. 5 agree with those found from the translational diffusion constant, D, $E_A \approx 500$ K at 1.46 g/cm^3 [25]. In this work, fits of D_{rot}, from τ_1 and τ_2, over 500 K$\geqslant T \geqslant$100 K give $E_A = 497$ K and $E_A = 525$ K, respectively. Since super-Arrhenius may have started for τ_2 at 100 K it is plausible to remove this point, yielding $E_A = 506$ K. The agreement of the different E_A is excellent given the uncertainties of the simulation.

The onset of super-Arrhenius in τ_l is somewhat ambiguous, and one might question whether the apparent deviation from Arrhenius behavior found at 100 K with τ_2 arises from a real change in the dynamics. This illustrates an essential point, that the usual analysis of relaxation times vs T provides limited, highly averaged information. A much better picture is provided by our new methods. In Fig. 6, the temperature-dependent distribution $P(\phi, \tau_c, T)$ reveals that

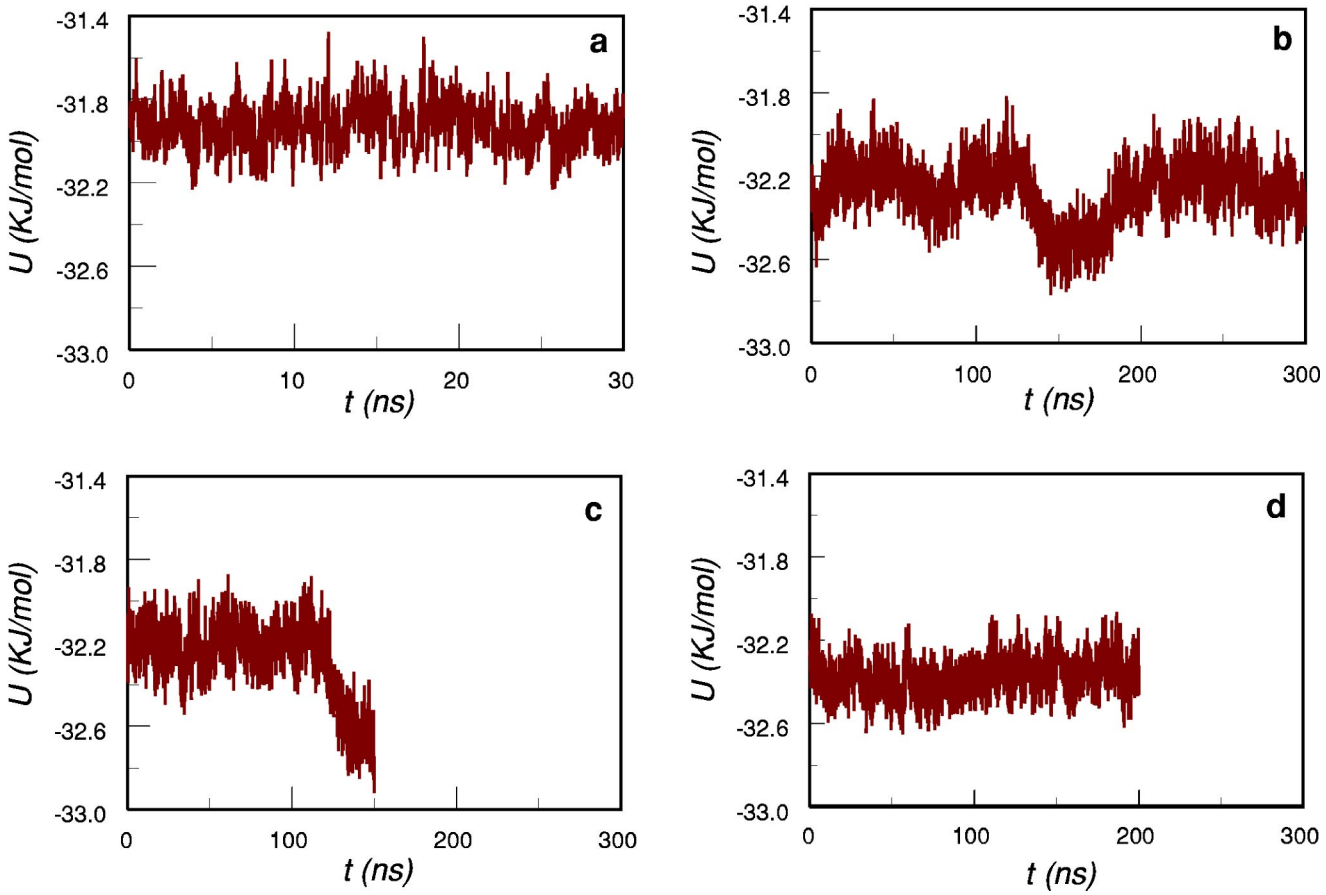

FIG. 9. Intermolecular part of the total potential energy, U, vs t for low-temperature trajectories; (a) 90 K, (b) 80 K run I, (c) 80 K run II, (d) 75 K.

heterogeneity is definitely present at 100 K, and even at 120 K a slight change from the high-temperature limit can be observed. This can be seen even more clearly in Fig. 6(c) with the indicator Δ_{het}. Here, we use 165 K as the reference temperature, and clearly at 100 K the heterogeneity is rising sharply. Thus the change from the high-T homogeneous dynamical mechanism starts at some intermediate T, surely above 100 K, where the deviation from Arrhenius behavior of an ensemble averaged quantity such as the relaxation time is obscure.

Now, we turn to the dynamic aspect or lifetime of rotational heterogeneity. An Arrhenius plot of the T-dependent exchange time τ_{ex}, calculated from $\Gamma_{het}(t_w)$, is shown in Fig. 7. Linear behavior crosses over to mild super-Arrhenius below about 100 K, as in the case of the rotational relaxation time (Fig. 5). Interestingly, the activation energy of τ_{ex} *exceeds* that of τ_c in the high-T linear regime. Fitting the data in Fig. 7 from 165 K to 120 K yields a slope about 680 K. These observations allow an explanation of how heterogeneity becomes important as T is decreased. At high T, the lifetime of heterogeneity is less than τ_c, and thus heterogeneity is not observed on the time scale of interest. Because of the different activation energies, however, τ_{ex} will overtake τ_c at a point below which heterogeneity persists on the time scale of α relaxation and becomes a dominant feature of dynamics. As seen in the 2D plots of $S(\phi_1,\phi_2,t_\omega)$ (Figs. 3, 4), at low temperatures the identity of slow molecules persists over the time scale of τ_c.

A broad crossover between distinct high-T and low-T dynamical mechanisms occurs as temperature is decreased in fragile liquids. The crossover may be described with two (or more) characteristic temperatures [30]. At T_A one can see the onset of collective behavior, and at the ''mode coupling temperature'' $T_c<T_A$ [31,32], $D(T)$ extrapolates to zero from above. Sastry *et al.* identified T_A as a temperature at which the T-dependent averaged *inherent structure* energy $\langle U_{is}(T)\rangle$—the energy of the local minima visited by the system—begins to decrease from its high-T plateau. At T_A they observed the onset of the nonexponential decay of the intermediate scattering function [33]. Kivelson and coworkers have introduced a crossover temperature associated with the presence of ''frustration limited domains'' [20]. Indeed, if we regard T_A as a temperature at which distinctive supercooled dynamics starts, criteria for T_A based upon different phenomenology just reveal different aspects of the crossover. The indicators of rotational heterogeneity introduced here are good candidates to identify T_A and we conclude that for CS_2, 1.46 g/cm^3, T_A lies above 100 K. We might draw the same conclusion from the clear presence of stretched exponential behavior (Table 2) at 100 K.

If the crossover begins at T_A, the low-T mechanism appears in full strength at T_c [34,35,13,36]. In terms of the

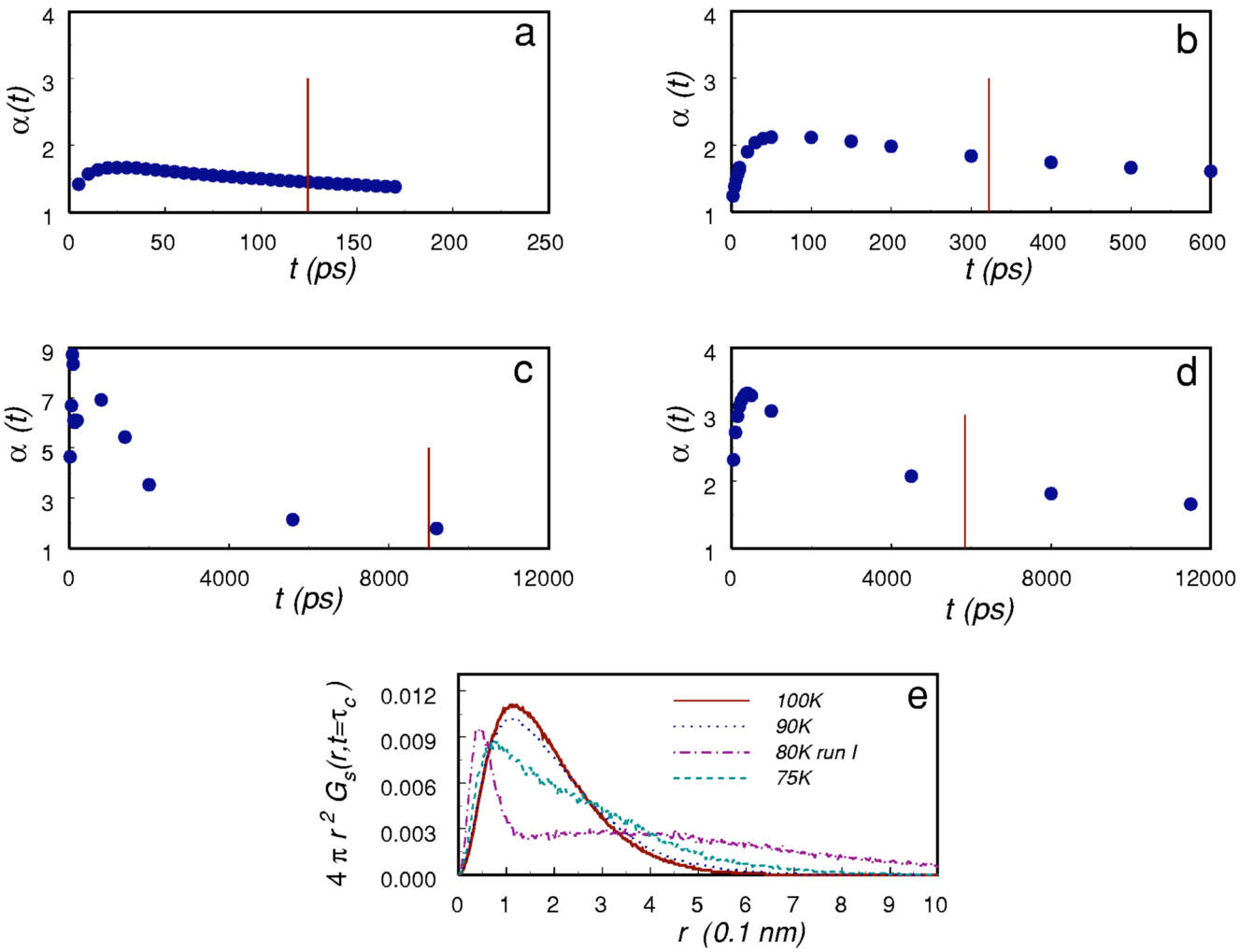

FIG. 10. Translational dynamics at low temperatures; (a)–(d), non-Gaussian parameter $\alpha(t)$ at 100 K, 90 K, 80 K run I, and 75 K, respectively. Time unit is picosecond and vertical line indicates τ_c. (e), van Hove distribution $P(r,t)$ at the same temperatures, r in Å.

landscape, the regimes $T>T_A$, $T_A>T>T_c$ and $T_c>T$ can be categorized as the high-temperature normal liquid, landscape influenced, and landscape dominated, respectively [33]. In this study, with the lowest temperatures, 80 K and 75 K, we attempt to observe phenomenological features relevant to the dynamical change around T_c. In Fig. 8, we estimate T_c with three different temperature ranges by fitting $D(T)$ to the power-law mode coupling formula. Fitting from 193 K to 85 K [Fig. 8(a)] gives $T_c=75.4\pm2.0$, from 165 K to 85 K [Fig. 8(b)] $T_c=71.6\pm2.8$, and 165 K to 90 K [Fig. 8(c)] $T_c=75.4\pm3.5$. The three slightly different estimates illustrate the uncertainties in determining T_c.

At 80 K and 75 K, close to T_c, the amplitude of rotational heterogeneity, measured by Δ_{het}, is (Fig. 6) increasing strongly. This supports the idea that the low-T mechanism is intertwined with heterogeneity. Figure 7 indicates that, in the noisy low-T data, τ_{ex} may be catching up to τ_c (requiring a breakdown of the high-T Arrhenius behavior, which would put the intersection at much lower T), another feature expected in heterogeneity-driven dynamics. Several other phenomena are apparent that are absent at high T. The first is that, while the supercooled state of CS_2 is very stable above 85 K, crystallization begins to be a problem below 85 K. In Fig. 9, we display the time dependence of the intermolecular potential energy; a sharp drop indicating crystallization is seen in in Fig. 9(c). At 80 K and 75 K, all trajectories ended with crystallization, and as a result the length of each run is not sufficient to give well averaged rotational quantities. In future work, we will investigate the possibility of approaching the minimum in the time to crystallization vs T, as observed in CO_2 [37]. Another point worth further study is the presence of long-lived correlated fluctuations in the potential energy. In Fig. 9(b) for 80 K, run I, there is a correlated fluctuation of over 50 ns.

Most simulations of supercooled liquids employ atomic models, so most discussions of T_c concern the translational dynamics. With CS_2, we may address the question of how the supercooled translational dynamics in molecular liquids compares to that of atomic systems. The relation between translation and rotation is an important aspect of the dynamical slowing down [1,16]. Translational motion is often viewed through the distribution $P(r,t)$ of atomic displacements at time t, where $P(r,t)=4\pi r^2 G_s(r,t)$ and $G_s(r,t)$ is the self-part of the van Hove correlation function. It has been

argued that a transition to a hopping mechanism, believed to occur below T_c, is signaled by the appearance of a second peak in $P(r,t)$ [33]. We suggest that a coupling of translation and rotation should be sought with $P(r,\tau_c)$, in states where rotational heterogeneity is clearly present. Also, translational heterogeneity has been investigated with the t-dependent non-Gaussian parameter [38,10],

$$\alpha(t)=\frac{2\langle r^4\rangle_t}{5\langle r^2\rangle_t}, \tag{11}$$

where $\langle\rangle_t$ represents an average with $P(r,t)$.

In Figs. 10(a)–(d) the non-Gaussian parameter is shown at 100 K, 90 K, 80 K (run I), and 75 K; a vertical line denotes $t=\tau_c$. With atomic liquids, Kob *et al.* found that the time for the maximum of $\alpha(t)$ increases as T decreases [10], and they explained this in terms of increasing heterogeneity; we find (Fig. 10) the same trend. The sharp peak [Fig. 10(c)] for 80 K (run I), shows that the heterogeneous translational dynamics is indeed associated with heterogeneous rotational dynamics. This finding is relevant to the breakdown of the Stokes-Einstein law observed experimentally at temperatures close to T_g, a topic for future work.

Figure 10(e) presents $P(r,\tau_c)$ at each temperature considered in Fig. 10(a)–(d). Just as $P(\phi,t)$ provides more information about rotational heterogeneity than $C_\phi(t)$, $P(r,t)$ is more informative than $\alpha(t)$. The shoulder seen in Fig. 10(e), 75 K, for $r\sim 3.75$ Å is preliminary evidence for hops occurring on the rotational time scale as $T\to T_c$ (and presumably below). This fits with the idea that an activated local rearrangement, which would correspond to a hop, is necessary for a molecule to reorient. The ratio τ_1/τ_2 has long been used to characterize, indirectly, the nature of molecular reorientation. In the small-step Debye limit of rotational diffusion

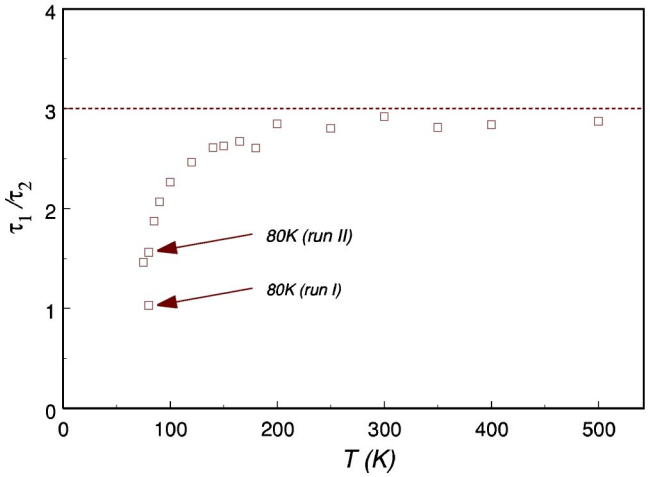

FIG. 11. T-dependent ratio τ_1/τ_2, $\rho=1.46$ g/cm^3. Two 80 K runs are indicated with arrows. Dotted line is the prediction of the Debye model.

$\tau_1/\tau_2=3$. The faster decay of τ_2, for the same molecular motion, is a simple consequence of P_2 having more zeros. On the other hand, for a mechanism of large reorientational jumps the density of zeros is irrelevant, and $\tau_1/\tau_2=1$. Figure 11 shows that the ratio has a high-T plateau close to 3, but begins to drop sharply below 150 K; run 1 at 80 K is actually ≈ 1. Again, the large change occurs in the vicinity of T_c. Our results suggest that reorientation in supercooled liquids requires local rearrangements leading to large angular jumps. With a computer simulation we can examine the individual molecular motions in much more detail. For Fig. 12(a) a molecule is randomly selected and the jump angles $\Delta\theta=\theta(t)-\theta(t-\Delta t)$ are displayed for points separated by $\Delta t=100$ ps$(\approx\tau_c/60)$ at 75 K. With the total jump angle

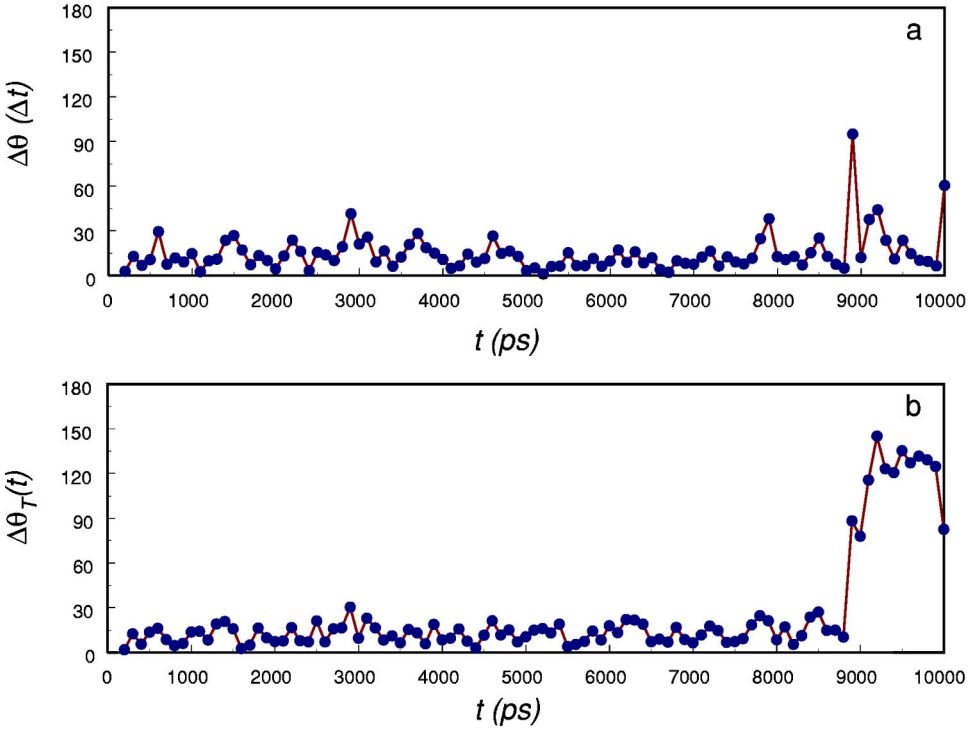

FIG. 12. Large angular jumps in a single molecular trajectory at 75 K, $\rho=1.46$ g/cm^3; (a), Angular changes (degrees) in time interval $\Delta t=100$ ps, $\Delta\theta=\theta(t)-\theta(t-\Delta t)$, (b) total angular changes (degrees) from initial time t_0, $\Delta\theta_T=\theta(t)-\theta(t_0)$.

$\Delta\theta_T = \theta(t) - \theta(t_0)$ plotted in Fig. 12(b), it is seen that the occurrence of infrequent large angular jumps is another property of deeply supercooled states. Investigations on the role of large angle jumps in deeply supercooled states are underway.

V. CONCLUSIONS AND PERSPECTIVES

We have introduced a new probe of rotational heterogeneity, the distribution $P(\phi,t)$, which is far more informative and sensitive than a conventional correlation function. Other authors have introduced higher-order correlations to study translational heterogeneity [22,23]. Knowing the distribution is equivalent to knowing all the moments, which are higher-order correlations. With $P(\phi,t)$ in hand other indicators, including a measure of the lifetime τ_{ex}, were constructed.

We tested our ideas with a simulation of supercooled CS_2, $\rho = 1.46$ g/cm^3. The simulation is of interest in itself, since almost all simulations of supercooled dynamics and/or heterogeneity have employed atomic models. A crossover from Arrhenius to super-Arrhenius behavior of the rotational correlation times was found, the necessary pattern for a fragile glass former.

Although no dynamical simulation can even come close covering the whole range from room temperature to T_g, we were able to characterize rotational heterogeneity down to T_c; its onset with decreasing T is clearly visible through $P(\phi,t)$. We have determined τ_{ex}, and we can explain how the heterogeneity is unimportant at high T and crucial at low T: the activation energy of τ_{ex} exceeds that of τ_c. Observation of a heterogeneous pattern in $P(\phi,\tau_c)$ might be a better way to identify the upper limit of the dynamical crossover, T_A, than the onset of super-Arrhenius in D, D_{rot}, or τ_l. For the second important crossover temperature we estimate $T_c \approx 75$ K.

As expected, several phenomena associated with the low-T mechanism manifest themselves as T_c is approached. These include rotational heterogeneity, the focus of this work, but also: (1) a shoulder in $P(r,\tau_c)$, indicating that translational rearrangements may cause the large rotational jumps; (2) the sharp fall of the ratio τ_1/τ_2 towards a value of unity, characteristic of a large jump mechanism; (3) sharp drop (Table II) in the stretched exponential parameter β; (4) the same behavior of the non-Gaussian parameter, indicative of translational heterogeneity, that has been found in atomic systems; (5) frequent crystallization; (6) long-lived correlated fluctuations of the potential energy. Thus we have demonstrated the relation of several aspects of molecular reorientation to the translational T_c, but much more simulation and theoretical work is needed to correlate all the diverse phenomena participating in the dynamical crossover. Finally, pursuing this strategy from the landscape point of view should provide further insights and will be the focus of our future work.

ACKNOWLEDGMENT

This work was supported by NSF Grant No. CHE0090975 and was benefited from discussions with J. Chowdhary.

[1] M.D. Ediger, Annu. Rev. Phys. Chem. **51**, 99 (2000).
[2] H. Sillescu, J. Non-Cryst. Solids **243**, 81 (1999).
[3] R. Böhmer, Curr. Opin. Solid State Mater. **3**, 378 (1998).
[4] L.A. Deschenes and D.A.V. Bout, Science **292**, 255 (2001).
[5] S.C. Glotzer and C. Donati, J. Phys.: Condens. Matter **11**, A285 (1999).
[6] B. Doliwa and A. Heuer, Phys. Rev. Lett. **80**, 4915 (1998).
[7] D. Thirumalai, R.D. Mountain, and T. Kirkpatrick, Phys. Rev. A **39**, 3563 (1989).
[8] H. Fynewever and P. Harrowell, J. Phys.: Condens. Matter **12**, 6305 (2000).
[9] R. Yamamoto and A. Onuki, Phys. Rev. Lett. **81**, 4915 (1998).
[10] W. Kob *et al.*, Phys. Rev. Lett. **79**, 2827 (1997).
[11] G. Johnson *et al.*, Phys. Rev. E **57**, 5707 (1998).
[12] G. Wahnstrom, Phys. Rev. A **44**, 3752 (1991).
[13] C.A. Angell, K.L. Ngai, G.B. McMillan, and S.W. Martin, Appl. Phys. Rev. **88**, 3113 (2000).
[14] C.D. Michele and D. Leporini, Phys. Rev. E **63**, 036702 (2001).
[15] S. Kämmerer, W. Kob, and R. Schilling, Phys. Rev. E **56**, 5450 (1997).
[16] M.T. Cicerone, P.A. Wagner, and M.D. Ediger, J. Phys. Chem. B **101**, 8727 (1997).
[17] R. Richert, J. Phys. Chem. B **101**, 6323 (1997).
[18] F.H. Stillinger and J.A. Hodgdon, Phys. Rev. E **50**, 2064 (1994).
[19] G. Tarjus and D. Kivelson, J. Chem. Phys. **103**, 3071 (1995).
[20] G. Tarjus, D. Kivelson, and P. Viot, J. Phys.: Condens. Matter **12**, 6497 (2000).
[21] C.A. Angell, B.E. Richards, and V. Velikov, J. Phys.: Condens. Matter **11**, A75 (1999).
[22] A. Heuer and K. Okun, J. Chem. Phys. **106**, 6176 (1997).
[23] S.C. Glotzer and C. Donati, J. Phys.: Condens. Matter **11**, A285 (1999).
[24] B.J. Berne and R. Pecora, *Dynamic Light Scattering* (Krieger, Malabar, 1990).
[25] W.-X. Li and T. Keyes, J. Chem. Phys. **111**, 328 (1999).
[26] B.M. Ladanyi and T. Keyes, J. Chem. Phys. **76**, 2047 (1982).
[27] D.J. Tildesley and P.A. Madden, Mol. Phys. **48**, 129 (1983).
[28] P. Moore and T. Keyes, J. Chem. Phys. **100**, 6709 (1994).
[29] K. Schulten *et al.*, *VMD Vol. 1.7: Visual Molecular Dynamics*, Theoretical Biophysics Group at the Beckman Institute of the University of Illinois.
[30] C.A. Angell, Nature (London) **393**, 521 (1998).
[31] U. Bengtzelius, W. Göetze, and A. Sjolander, J. Phys. Chem. **29**, 2765 (1984).
[32] W. Göetze, in *Liquids, Freezing and the Glass Transition*, edited by J.P. Hansen, D. Levesque, and J. Zinn-Justin (Elsevier, New York, 1991).

[33] S. Sastry, P.G. Debenedetti, and F.H. Stillinger, Nature (London) **393**, 554 (1998).
[34] M. Goldstein, J. Chem. Phys. **51**, 3728 (1969).
[35] M.D. Ediger, C.A. Angell, and S.R. Nagel, J. Phys. Chem. **100**, 132000 (1996).
[36] P.G. Debenedetti and F.H. Stillinger, Nature (London) **410**, 259 (2001).
[37] I.M. Svishchev and P.G. Kusalik, Phys. Rev. Lett. **75**, 3289 (1995).
[38] A. Rahman, Phys. Rev. **136**, A405 (1964).